Ultrafast measurement of the optical properties of aluminum during shock-wave breakout

David J. Funk, D. S. Moore, K. T. Gahagan, S. J. Buelow, J. H. Reho, G. L. Fisher, and R. L. Rabie
Los Alamos National Laboratory, Los Alamos, New Mexico 87545
(Received 14 May 2001; published 31 August 2001)

We have used high-resolution frequency domain interferometry to make ultrafast measurements of shock-induced changes in the optical properties of thin aluminum targets. Measurements with an 800 nm probe wavelength found an unexpected phase shift during a 4.65 GPa shock breakout. Further measurements at 400 nm associate this phase shift with the pressure dependence of the 1.5 eV interband transition in aluminum. Data taken at several angles of incidence allowed the separation of optical from material motion effects, yielding an effective complex index for the shocked material.

DOI: 10.1103/PhysRevB.64.115114 PACS number(s): 78.20.Ci, 47.40.Nm, 62.50.+p

INTRODUCTION

Aluminum is considered to be the simplest nearly free electron (NFE) metal. As such, local pseudopotential models have been used to describe its experimental high-pressure properties and are in good agreement with more sophisticated theoretical models for the electronic structure at reduced volume.[1] These models have been used successfully to interpret spectroscopic data at high static pressure and temperature.[2,3]

Absorption peaks in polyvalent metals may arise when the Fermi surface cuts the Brillouin Zone (BZ) faces.[4] In general, an absorption edge is expected for each face that is cut and the position of the edge will occur at a photon energy equal to the energy gap appropriate to the particular zone plane. At the BZ boundary in the NFE band structure of fcc Al, the first and second bands are split by an amount determined by the absolute value $U(G)$ of the relevant Fourier coefficient of the potential. A pair of bands is almost parallel in BZ planes perpendicular to the two directions Γ-L and Γ-X. The fact that the Fermi surface cuts through these BZ faces, coupled with the parallelism of these bands, results in van Hove singularities of the unbroadened joint density of states for direct optical transitions at energy $2U(G)$. Because of differences in the density of states, the $2U(111)$ transition at 0.4 eV is weaker than the $2U(200)$ transition at 1.5 eV. Optical reflectivity and absorption measurements show a clearly resolved minimum at 1.5 eV, but the 0.4 eV feature is masked by the strong Drude-type optical response. Both the static pressure and temperature dependences of the 1.5 eV interband transition have been studied. Tups and Syassen found a pressure-dependent shift of $4.35 \pm 0.3\,\mathrm{meV\,kbar^{-1}}$.[2] The temperature variation was found to be consistent with the expected influence of the Debye-Waller factor and volume changes, and is negligible over the temperature range of the experiments reported here.[3]

The technique of frequency domain interferometry has been used to characterize the rise of the free surface particle velocity as a shock wave exits a target material.[5] The measurements in thin Al films that used a probe wavelength near 800 nm were influenced by an unexpected phase shift during shock breakout. We report results of experiments that support the association of this effect with the pressure-dependent shift of the $U(200)$, 1.5 eV, interband transition in Al.

EXPERIMENT

In this experiment, we employed the technique of reflection frequency domain interferometry (FDI) (Refs. 6,7) to simultaneously measure the dynamic phase shift between a pair of ultrafast probe pulses during shock breakout from thin-film Al targets. Details of the experimental approach can be found in Ref. 5. A single 800 nm, 130 fs, 0.7 mJ laser pulse generated by a seeded, chirped pulse amplified Ti:sapphire laser system (Spectra Physics) was used for both shock generation and probing. The shock generating (drive) pulse (0.2–0.5 mJ) was focused through the BK-7 portion of the target assembly onto the vapor-deposited Al to a diameter of $d_s = 75\,\mu$m. We have found that nonlinear absorption (optical breakdown) and possibly other nonlinear effects (Kerr focusing) in the BK-7 lead to a clipping of the pulse intensity, resulting in top-hat intensity profiles that generate extremely planar shock waves (0.7 nm rms over a 75 μm diameter spot).[8] A small portion of the main pulse ($\sim$0.04 mJ) reflected from a beam splitter was passed through an unbalanced Michelson interferometer to produce a pair of probe pulses separated in time by 4–12 ps. These pulses were focused onto the backside of the target at angles of $\theta = 32.6°$, 82.5°, or 84.5° (the data were sometimes taken at two angles simultaneously), to a diameter of $\sim$200 μm which circumscribed the region of shock break out. A doubling crystal was optionally inserted before interaction with the target to probe at 400 nm. Probe wavelengths at 770, 800, and 839 nm were generated by tuning the wavelength of the Ti:sapphire laser system. In all cases, the probe intensity was less than $\sim 5 \times 10^{11}\,\mathrm{W/cm^2}$. The reflected probe pulses were imaged at $\times$16 magnification onto the entrance slit of a high resolution imaging spectrograph (Acton model 300*i*) with CCD detector (Photometrics model SenSys 1600). The incidence polarization angle of the probe pulses was adjusted using a multiple order half-wave plate in combination with a Glan-Taylor polarizer.

The experiments reported here measured the phase difference between a pair of probe pulses initially produced by the unbalanced Michelson. Reflection of these pulses from an accelerating metallic surface (due to the emerging shock wave) will yield a phase shift that depends on time and the relative positions of the probe beams with respect to the onset of acceleration. The details of the data analysis used to

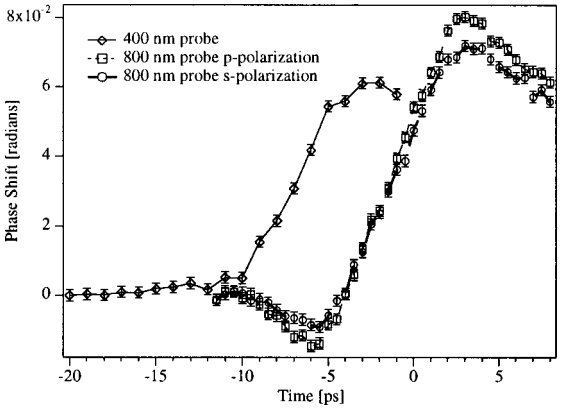

FIG. 1. Plot of measured phase difference between the probe beams vs relative delay (to the pump laser) for shock-wave breakout from a 1000-nm-thick Al thin film. Note the absence of the negative phase shift in the 400-nm data (the data sets are offset in time for clarity) and the increase in negative phase shift with *p*-polarized light vs *s*-polarized light at 800 nm.

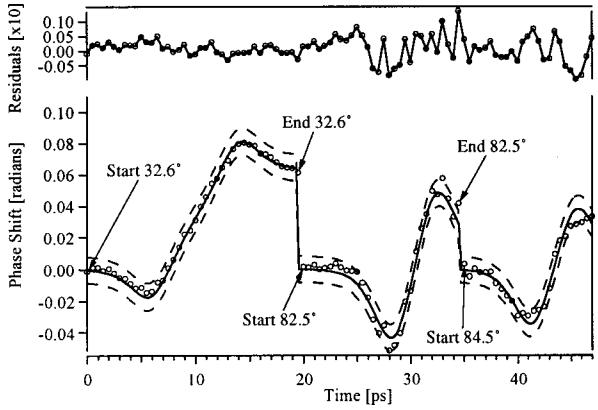

FIG. 2. Plot of measured phase difference between the probe beams vs relative delay (to the pump laser) for a shock-wave breakout from a 750-nm-thick Al thin film. The probes are *p*-polarized 800-nm light taken at three angles of incidence (which are offset in time for clarity). Note the maximum negative phase difference occurs in the data taken near the quasipolarizing angle in aluminum (82.5°). The dashed lines are 95% confidence limit prediction bands.

extract the relative phase shift between the probe pulses caused by motion of the surface or transient changes in the optical properties of the sample during shock breakout are given in Ref. 5. The phase data were extracted over the center $\sim 50\ \mu$m of the planar shocks.

The targets used in this experiment were Al films of ~ 750 and ~ 1000 nm thickness produced by vapor deposition onto $150+/-20\ \mu$m thick BK-7 microscope cover slips (Fisher Scientific). The samples were examined both with a spectroscopic ellipsometer (Sentech SE 800) and an atomic force microscope (AFM; Quesant Nomad). Best fits to the spectral ellipsometric data from the 750 nm Al sample [Ψ and Δ measured over 400–840 nm (Ref. 9)] modeled as an Al_2O_3 layer on top of the aluminum substrate yielded an Al_2O_3 layer 4.9-nm thick, consistent with literature results.[10] This thickness was used in subsequent data analysis and hydrocode simulations. AFM results indicated an rms roughness of ~ 5 nm over a 900 μm^2 area, consistent with the ellipsometric data, in which Ψ was fit less satisfactorily than Δ.

RESULTS

Figure 1 shows the relative phase shift as a function of delay time between the shock generation pulse and the probe pulses for a 1000-nm-thick Al film measured using a probe wavelength of 800 nm, probe pulse separation of 8 ps, and both *s* and *p* polarization. Each data point is the average of ten shots and the spacing between data points is 0.5 ps. The experiments done at 771 and 839 nm gave results equivalent to those at 800 nm within the error limits. The *negative* phase shift that occurs during shock breakout is very apparent and unexpected. We use the convention in our data analysis that material motion alone would yield a *positive* phase shift. It can also be seen that the *p*-polarization data contains a significantly larger negative phase shift than the *s*-polarization data. Also shown in Fig. 1 is the identical sample under similar conditions, but with a probe wavelength of 400 nm and probe pulse separation of 4 ps. No experiment done with the probe wavelength at 400 nm resulted in an observable negative phase shift during shock breakout. Finally, in Fig. 2 we show three sets of data using the 750-nm-thick Al sample (and their fits, see below) all taken with an 800 nm *p*-polarized probe but at different angles of incidence and temporal separations (32.6°, 8 ps; 82.5°, 4 ps; 84.5°, 4 ps). As will be shown, at high angles of incidence the signal is dominated by changes in the complex index of refraction, with a small contribution resulting from the surface motion.

DISCUSSION

Reflection from an air-metallic interface is governed by Maxwell's equations and appropriate boundary conditions leading to the Fresnel relations for the reflection amplitudes of *s*- and *p*-polarized light:[10,11]

$$r_s=\frac{-\sin(\theta_0-\theta_1)}{\sin(\theta_0+\theta_1)}=\rho_s e^{i\phi_s},\quad r_p=\frac{\tan(\theta_0-\theta_1)}{\tan(\theta_0+\theta_1)}=\rho_p e^{i\phi_p}, \tag{1}$$

where θ_0 is the angle of incidence in air and θ_1 is the complex angle of incidence in the metal as determined from Snell's law and the metal's complex index. Thus, upon reflection from a stationary metallic surface, the electric field undergoes a phase shift ϕ_n with magnitude ρ_n, that can be accurately calculated from knowledge of the complex index of refraction, polarization state, and the angle of incidence of the light striking the sample. Moreover, this phase shift will be influenced by any time-dependent changes in the complex index of refraction of the material, through the resulting changes in the phase shifts calculated with Eq. (1), as the pressure wave approaches the surface and subsequently accelerates it. Thus, we initially ascribe the differences in the *s*- and *p*-polarized 800 nm probe data and the 400 nm probe data to relative differences in the calculated phase shifts from

TABLE I. Parameters determined from fits to the data shown in Fig. 1, along with measured and calculated values for the complex index.

	This work, 800 nm, 4.65 GPa	This work, 400 nm	(Refs. 1 and 17) 4.65 GPa	Ambient (Refs. 1 and 17)	UHV (Ref. 10)
τ	2.36 ± 0.09 ps	2.32 ± 0.40 ps			
u_p	0.300 ± 0.006 nm/ps	0.29 ± 0.02 nm/ps			
n	1.56 ± 0.20		1.79	2.35	2.798
k	8.29 ± 0.04		6.68	7.80	8.446

Eq. (1), resulting from the pressure induced shift of the $U(200)$ interband transition in aluminum.

To both account for and quantify the influence of changes in the complex index, we modeled the data taken at 800 nm with *p*-polarization and multiple angles of incidence. In addition to the data taken at 32.6° incident angle, data were taken at large incident angles to maximize the effect of the complex index changes, which occurs near the quasipolarizing angle (near 82.5° in aluminum). Measurement at large incident angles minimized the contribution of the phase signal due to surface motion, which is proportional to the cosine of the angle of incidence [see Eq. (2)], effectively separating the two effects. We assumed that the free surface velocity's time dependence was adequately described by a hyperbolic tangent function as in Ref. 5. We then took the changes in the complex index to be proportional to the acceleration of the surface, which is related to the pressure.

In the case of aluminum, in which an Al_2O_3 layer always exists on the surface, the acceleration is complicated by the presence of the overlayer, which enhances the optical effects. CTH (Refs. 12 and 13) hydrodynamic calculations of an aluminum film indicate that, without the $\sim$5 nm Al_2O_3 overlayer, the pressure 1–2 nm below the surface never exceeds 0.1–0.2 GPa. In contrast, inclusion of 4.9 nm Al_2O_3 overlayer in the calculation and the resulting shock impedance mismatch allows the aluminum surface to approach the 4.65 GPa pressure (inferred from the free surface velocity and Al Hugoniot[14]) behind the shock front. Since aluminum's skin depth is very small, $\sim$15 nm, the influence of pressure-induced complex index changes will be much greater with the overlayer than without.

Finally, to extract an *n*-effective (n_{eff}) and *k*-effective (k_{eff}), and to account for the Al_2O_3 overlayer in phase shift calculations, we treated the overlayer aluminum as a thin film in which *only* the complex index of the aluminum is time dependent. We set and did not vary the index of the Al_2O_3 layer ($n=1.76$, $k=0$) to literature values[15] and we fixed the layer thickness at 4.9 nm. This choice is consistent with the facts that the index of sapphire changes very little under moderate shock conditions [$<$12.0 GPa (Ref. 16)] and that the compression the sapphire undergoes due to the shock wave (less than 2% or 0.1 nm) causes a phase shift less than the noise in our method [0.7 nm rms (Ref. 5)]. Then, the three data sets were fit simultaneously to the differences of the following equation for the time-dependent phase shift of each probe:

$$\phi_j(t)=\Delta\phi_{n,n_{\mathrm{eff}},k,k_{\mathrm{eff}}}\,\mathrm{sech}^2\left(\frac{t-t_j+\delta t_j}{\tau}\right)+\frac{4\pi\cos(\phi_0)}{\lambda_0}\int_{t_i}^{t_t}u_p\left[1+\tanh\left(\frac{t-t_j+\delta t_j}{\tau}\right)\right]dt, \tag{2}$$

where ϕ_j is the phase shift for probe pulse j, $\Delta\phi$ is determined by taking the difference in phases from Eq. (1) (using, $n,k,n_{\mathrm{eff}},k_{\mathrm{eff}}$) and λ_0 is the wavelength. δt_j is determined from the temporal delay introduced by the interferometer. The following parameters were varied: $\tau,u_p,t_j,n_{\mathrm{eff}},k_{\mathrm{eff}}$, where τ is the hyperbolic tangent time constant, u_p is the shock state particle velocity, t_j are offsets for the data from each set (time relative to the pump, which can change from day to day), and n_{eff} and k_{eff} are the effective complex index of shocked aluminum. Nonlinear least squares analysis (Levenberg-Marquardt, Igor Pro 4, Wavemetrics) yielded the parameters in Table I. Also included are the parameters obtained by fitting the 400-nm probe data from the 1000-nm-thick film sample using Eq. (2) but without the optical contribution, along with the predicted *n* and *k* from Refs. 1 and 17 and experimentally derived ambient values.[15] Fits to the 800-nm data are shown in Fig. 2, along with the residuals and 95% confidence limit prediction bands. Note that the residuals are larger for data taken at the high angles of incidence, which had a much lower S/N ratio due to larger shot-to-shot pointing errors.

A comparison of time constants τ from data taken at the two probe wavelengths of 400 and 800 nm show that they are the same within statistical error, which is satisfying, since the shock-wave rise time should be independent of the optical effects. Also listed are the n_{eff} and k_{eff} extracted from the fit. We have used Sturm and Ashcroft's model,[1] with the modified parameters introduced in Ref. 17 to calculate *n* and *k* as a function of pressure at 800 nm, which is affected by the shift in position of $U(200)$. We note that their model does an excellent job of calculating reflectivities at a diamond/aluminum interface when compared to those measured in Ref. 2. Note that the absolute magnitudes of the changes in the complex index are different, but the trends are in the correct direction. Thus, we conclude that our data are being influenced by the pressure-dependent shift of the $U(200)$ interband transition in aluminum. However, our model yields an *effective* complex index. Physically, one expects that the pressure wave moving forward in the material will vary the index smoothly from low pressure to high. Our

model assumes that a single index exists for the aluminum substrate as the wave moves forward. We have tried modeling the layer with two additional schemes: (1) the shock wave is infinitesimally sharp, making the surface look like a time-dependent thin film of three layers Al_2O_3, Al, and shocked Al and (2) the shocked layer is described with an index gradient, with a pressure profile given by the acceleration history that moves forward in time. The second scheme necessitated modeling of the shocked/nonshocked aluminum as a large number of layers, as is typically done in modeling a complex film.[18] In all three cases, the data were fit sufficiently well so that distinction on χ squared was not possible. However, we believe the effective model is the most accurate and also most relevant to use, since experiments that might use this information, i.e., shock temperature measurements from optical emission, only need the effective index as a function of time. Moreover, our observations may include some smearing of the breakout due to surface roughness, which will be better captured by an effective model. Thus we have chosen to report n_{eff} and k_{eff} as derived from this model.

Finally, we note that we have also taken data with nickel substrates (Fig. 3) at three angles of incidence.[19] In the case of nickel, we found the observed optical contributions are of the opposite sign as those for aluminum, indicating that the nickel data taken at 32.6° will contain an optical phase contribution in the same direction as surface motion. However, in contrast to aluminum, this may be interpretable in terms of a Drude response, as nickel has no interband transition near 800 nm. We note that the absolute position of the surface derived from these measurements will be in error if the optical effects are not taken into account.

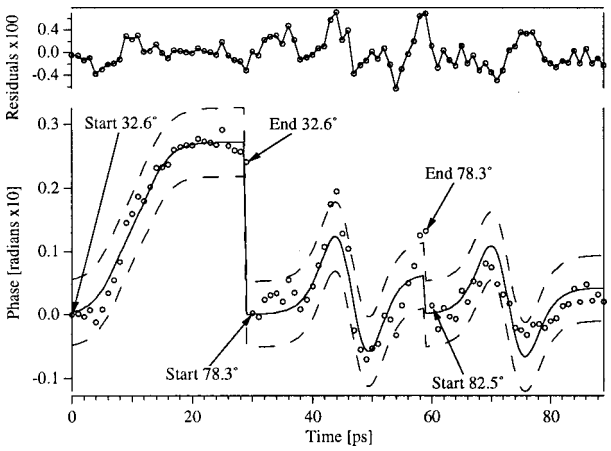

FIG. 3. Plot of measured phase difference between the probe beams vs relative delay (to the pump laser) for shock-wave breakout from a 500-nm-thick Ni thin film. The data were obtained using *p*-polarized 800-nm light and taken at three angles of incidence (which are offset in time for clarity). Note the large positive phase difference in the data taken near the quasipolarizing angle in nickel (78.3°), indicating significant complex index changes leading to phase differences of the same sign as those from surface motion. The dashed lines are 95% confidence limit prediction bands.

CONCLUSION

An unexpected phase shift found in frequency domain interferometric measurements of laser shocked thin film aluminum samples has been investigated. The lack of such a feature using a 400 nm probe wavelength, as well as the polarization and incident angle dependence of the strength of the feature, provide support for it being the result of the pressure-dependent shift of the $U(200)$ interband transition in aluminum. The complex index of refraction values extracted from fits to the data are consistent with optical conductivities reported from static high pressure and calculational studies at the pressure given by the final particle velocity in these experiments. We note that FDI measurements at a single angle of incidence may yield erroneous position vs. time data, due to the influence of changes in the optical constants of the shocked material if such changes are not taken into account.

ACKNOWLEDGMENTS

This work was performed at Los Alamos National Laboratory by the University of California under the auspices of the U.S. Department of Energy under Contract No. W-7405-ENG. We also acknowledge the generous trust and support of Joe Repa, Alan Picklesimer, and Judith Snow.

[1] N. W. Ashcroft and K. Sturm, Phys. Rev. B **24**, 2315 (1981).
[2] H. Tups and K. Syassen, J. Phys. F: Met. Phys. **14**, 2753 (1984).
[3] A. G. Mathewson and H. P. Myers, J. Phys. F: Met. Phys. **2**, 403 (1972).
[4] N. W. Ashcroft and N. D. Mermin, *Solid State Physics* (Saunders College, 1976).
[5] K. T. Gahagan, D. S. Moore, David J. Funk, R. L. Rabie, S. J. Buelow, and J. N. Nicholson, Phys. Rev. Lett. **85**, 3205 (2000).
[6] E. Tokunaga, A. Terasaki, and T. Kobayashi, Opt. Lett. **17**, 1131 (1992).
[7] J. P. Geindre *et al.*, Opt. Lett. **19**, 1997 (1994).
[8] D. S. Moore, K. T. Gahagan, J. H. Reho, David J. Funk, S. J. Buelow, R. L. Rabie, and T. Lippert, Appl. Phys. Lett. **78**, 40 (2001).
[9] Ψ is defined as the tangent inverse of the ratio of *s*-polarization reflectance amplitude to *p*-polarization reflectance amplitude. Δ is defined as the difference in phase shift upon reflection, see Eq. (1), between *s* and *p* polarizations.
[10] D. Y. Smith, E. Shiles, and M. Inokuti, in *Handbook of Optical Constants of Solids*, edited by E. D. Palik (Academic, San Diego, 1985), p. 374.
[11] See, for example, J. M. Bennett, in *Handbook of Optics I*, edited by M. Bass, E. W. Van Stryland, D. R. Williams, and W. L. Wolfe (McGraw-Hill, New York, 1995), Chap. 5.
[12] J. M. McGlaun *et al.* (unpublished).
[13] Clearly, using a continuum code on a scale that approaches the atomic will yield qualitative results, but it is very useful for physical insights.

[14] *LASL Shock Hugoniot Data*, edited by S. P. Marsh (University of California Press, Berkeley, 1980), p. 182.
[15] F. Gervais, in *Handbook of Optical Constants of Solids II*, edited by E. D. Palik (Academic, San Diego, 1991), p. 761.
[16] L. M. Barker and R. E. Hollenbach, J. Appl. Phys. **41**, 4208 (1970).
[17] R. G. Dandrea and N. W. Ashcroft, Phys. Rev. B **32**, 6936 (1985).
[18] See, for example, R. M. A. Azzam, in *Handbook of Optics II*, edited by M. Bass, E. W. Van Stryland, D. R. Williams, and W. L. Wolfe (McGraw-Hill, New York, 1995), Chap. 27.
[19] David J. Funk, D. S. Moore, K. T. Gahagan, J. H. Reho, S. J. Buelow, G. L. Fisher, and R. L. Rabie (unpublished).